Localized interface optical-phonon modes in graded 3*C*-SiC/Si heterojunctions

R. C. Vilela,[1] R. N. Costa Filho,[1] E. F. Nobre,[1] V. N. Freire[1], and E. L. Albuquerque[2,*]
[1]*Departamento de Física, Universidade Federal do Ceará, Caixa Postal 6030, 60455-900 Fortaleza, Ceará, Brazil*
[2]*Departamento de Física, Universidade Federal do Rio Grande do Norte, 59072-970 Natal-RN, Brazil*
(Received 29 October 2002; revised manuscript received 25 March 2003; published 15 July 2003)

We study the properties of localized interface optical-phonon modes in Si/3*C*-SiC heterojunctions within the framework of the dielectric continuum theory. Our model calculation takes into account the existence of an interfacial nonabrupt transition region, whose thickness is considered varying from 0.5 to 2.5 nm. Numerical results reveal some interesting properties of the interface effects, which can substantially shift (up to 20 cm^{-1}) the high-frequency antisymmetric interface modes found in the abrupt case. Moreover, optical-phonon modes emerge in the low-frequency range of the spectrum, which are sensitive to the value of the nonabrupt interface thickness.

DOI: 10.1103/PhysRevB.68.033307 PACS number(s): 78.66.Sq, 78.20.−e

The investigation of phonons in nanostructures has been very important in the last two decades due to the fundamental physical concepts employed to describe their intrinsic properties as well as for their potential device applications (for a review see Refs. 1,2). Tailoring of optical phonon modes in nanoscale semiconductors was proposed, suggesting that confined phonon effects can be used to tune quantum-well intersubband lasers.[3] The control of phonon scattering mediated intersubband transitions affect laser properties critically. Phonon modes engineering was proposed to be achieved by inserting a single alloy semiconductor step, producing three-interface heterostructures[4] as well as step quantum well structures.[5] However, the existence of micro-roughness superimposed to macroroughness gives rise to the existence of graded interfaces in semiconductor heterostructures. Even in systems such as $GaAs/Al_xGa_{1-x}As$, the thickness of the graded interface regions is at least of the order of three monolayers, which is enough to have an effect on the laser optical gain, for example.[6] Consequently, it is important to investigate the role of naturally occurring graded interface on the phonon modes of semiconductor heterostructures.

Progress in microfabrication techniques enables us to create various kinds of hetero-epitaxial interfaces between two dissimilar and yet closely lattice-matched semiconductors and facilitate the dramatic reduction in extrinsic interface defects detrimental to the electron mobility and other device parameters. In such heterojunctions, since experimental reality is approaching theoretical models and assumptions, detailed analysis and precise predictions are unprecedentedly made possible.[7] This is particularly true in the case of 3*C*-SiC/Si(100) heterojunctions, which are very promising for the fabrication of resonant tunneling diodes for high-speed and high-power applications. Successful growth of 3*C*-SiC(100) thin films on Si(100) has been achieved by many groups mainly by chemical vapor deposition[8–11] and molecular ion beam deposition.[12] In particular, the existence of transition regions with thickness at least equal to 1 nm was found by high-resolution transmission electron microscopic observation in 3*C*-SiC/Si(100) heterojunctions, which were recently grown using a chemical vapor deposition technique with pulsed supersonic free jets.[11]

Raman scattering measurements have been used to study both residual and strain relaxation effect at the 3*C*-SiC/Si interface.[13–16] By investigating the TO- and LO-phonon Raman scattering, both theoretically and experimentally, it was found that different strain regimes do coexist. The fluctuating strain induces both inhomogeneous broadening and a shift smaller than 5 cm^{-1} of the Raman line (both LO and TO modes).[14,15] Furthermore, strong interface-induced changes on the Raman scattering in 3*C*-SiC/Si superlattices was recently previewed by theoretical calculations.[17] The main influence of the nonabrupt interface was the appearance of new peaks in between those related to the Si-quasiconfined and 3*C*-SiC-confined modes. Examination of atomic displacements allowed for the effects to be tracked as localization or delocalization of the vibrations.

Optical vibration properties in heterojunctions were extensively investigated both theoretically[18] and experimentally[19] during the past two decades. In particular, the interface optical-phonon modes have been found to play a dominant role in electron-phonon interactions in quantum wells and superlattices.[20] Considering a 3*C*-SiC/Si superlattice with sharp interfaces, it is well known that its localized optical-phonon modes have two branches bounded by the longitudinal (LO) and transverse (TO) bulk optical-phonon modes of the SiC, whereas the presence of inhomogeneities such as surface, interface, or defect layers obviously will change this spectrum. To date, the interface modes in semiconductor systems were calculated only within the assumption of sharp interfaces between their constituents.

It is the aim of this paper to investigate the effect of an interfacial transition region on the optical-phonon modes spectra in a 3*C*-SiC/Si heterojunction. According to the high-resolution transmission electron microscopy observations of Ikoma *et al.*,[11] the transition regions in Si/3*C*-SiC/Si(100) multilayer systems have a thickness of the order of 1 nm, with a root-mean-square roughness of 2.8 nm. Considering that the use a buffer layer technique[21,22] or carbonization step[23] for 3*C*-SiC/Si heteroepitaxy is very promising for reducing defects in this system, the 3*C*-SiC/Si nonabrupt interface region is considered in this work to be formed by a $(3C\text{-SiC})_x(\text{Si})_{1-x}$ layer. Here x decreases monotonically from 0 to 1 through the nonabrupt interface

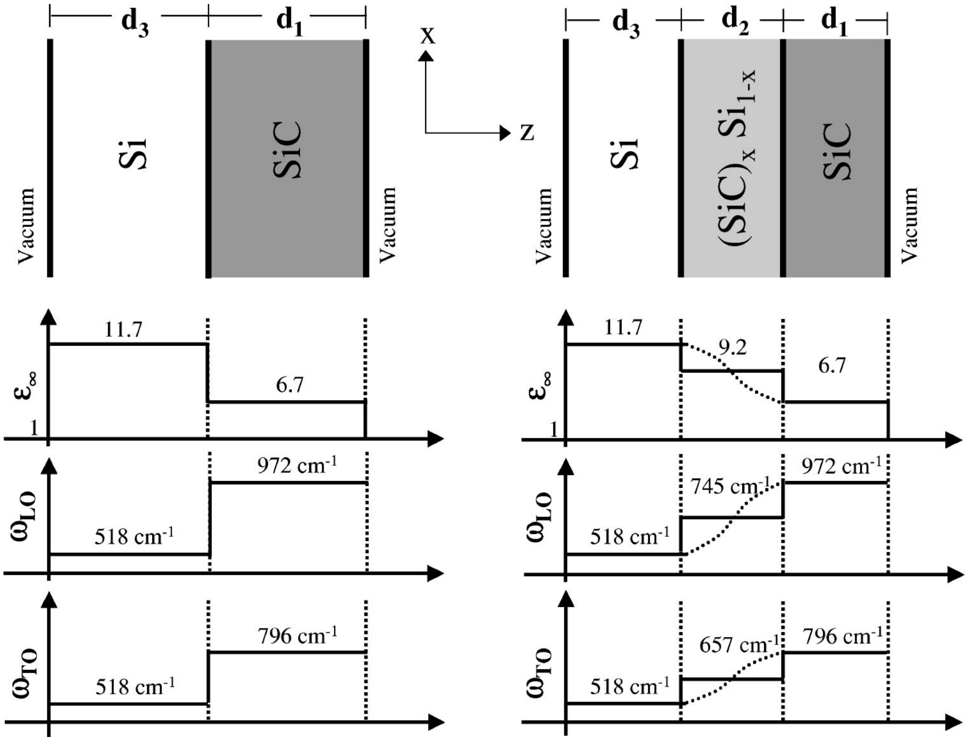

FIG. 1. Schematic representation of an abrupt $3C$-SiC/Si (left-hand side) and nonabrupt Si/Si$_x$($3C$-SiC)$_{1-x}$/$3C$-SiC (right-hand side) heterojunction.

region (x tends to zero in the Si side, and tends to one in the SiC side), giving rise to a continuous variation of ϵ_∞, ω_{LO}, and ω_{TO} (see dotted lines in Fig. 1). Furthermore it is considering that $\epsilon_\infty = 9.2$, $\omega_{\mathrm{LO}} = 745\ \mathrm{cm}^{-1}$, and $\omega_{\mathrm{TO}} = 657\ \mathrm{cm}^{-1}$ in the $(3C\text{-SiC})_x(\mathrm{Si})_{1-x}$ interface region, assuming an interpolation of the high-frequency dielectric constants and phonons frequencies of Si and $3C$-SiC. This imply that in this model the nonabrupt interface is a single $(3C\text{-SiC})_x(\mathrm{Si})_{1-x}$ step, which is clearly shown in Fig. 1.

A macroscopic theory, based on the dielectric continuum model together with a matrix-transfer treatment to simplify the algebra, which is otherwise quite complicated, is used to calculate the dispersion relation for the optical phonon, which fulfills electrostatic boundary conditions and allows one to obtain analytical expressions for the phonon dispersion relation. Within this model, the optical-phonon modes in the no-retardation limit satisfy the classical electrostatic equations, i.e.,

$$\vec{E}(\vec{r}) = -\nabla\phi(\vec{r}), \tag{1}$$

$$\vec{D}(\vec{r}) = \vec{E}(\vec{r}) + 4\pi\vec{P}(\vec{r}) = \epsilon_\perp(\omega)E_\perp(\vec{r})\hat{\rho} + \epsilon_z(\omega)E_z(\vec{r})\hat{z}, \tag{2}$$

$$\nabla\cdot\vec{D}(\vec{r}) = 0, \tag{3}$$

where $\phi(\vec{r})$ is the electrostatic potential due to the optical-phonon mode, $\vec{E}(\vec{r})$ is the electrical field, $\vec{D}(\vec{r})$ is the displacement field, $\vec{P}(\vec{r})$ is the polarization field, and $\hat{z}$ ($\hat{\rho}$) denotes the unit vector along the z (xy plane) direction. The direction-dependent dielectric functions $\epsilon_\perp(\omega)$ and $\epsilon_z(\omega)$, which play important role in Raman scattering experiments,[17] are given by

$$\epsilon_\perp(\omega) = \epsilon_{\perp\infty}\frac{\omega^2-\omega_{\perp\mathrm{LO}}^2}{\omega^2-\omega_\perp^2}, \tag{4}$$

$$\epsilon_z(\omega) = \epsilon_{z\infty}\frac{\omega^2-\omega_{z\mathrm{LO}}^2}{\omega^2-\omega_z^2}, \tag{5}$$

where $\omega_\perp$ (ω_z) is the lattice dispersion frequency, and $\omega_{\perp\mathrm{LO}}$ ($\omega_{z\mathrm{LO}}$) is the longitudinal-optical (LO) phonon frequency. Also, $\epsilon_{\perp\infty}$ ($\epsilon_{z\infty}$) is the high-frequency dielectric constant perpendicular (along) the z axis. We assume here that the relation $\epsilon_{\perp\infty} = \epsilon_{z\infty} = \epsilon_\infty$ is satisfied with good accuracy.

Considering now the phonon potential of the form $\phi(\vec{r}) = \phi(z)\exp(i\vec{q}\cdot\vec{\rho})$, where $\vec{q}$ is the two-dimensional phonon wave vector, its equation of motion is[24]

$$\nabla\cdot\vec{D} = [\epsilon_\perp(\omega)q^2 - \epsilon_z(\omega)\partial^2/\partial z^2]\phi(r) = 0. \tag{6}$$

This electrostatic potential is related to the localized interface optical-phonon modes, and exhibits oscillatory decay behavior inside the heterojunction, with all peaks and valleys located at the interfaces. These properties may be attributed to the fact that the structure considered here is symmetrical.

Using Maxwell standard boundary conditions, namely the continuity of the z component of the displacement vector $\vec{D}$ and the tangential component of the electrical field $\vec{E}$ at the interfaces of the $3C$-SiC/$(3C\text{-SiC})_x(\mathrm{Si})_{1-x}$/Si heterojunction of thickness $L = L_{3C\text{-SiC}} + L_{(3C\text{-SiC})_x(\mathrm{Si})_{1-x}} + L_{\mathrm{Si}} = d_1 + d_2 + d_3$, we obtain, after a bit of algebra, the following expression for the phonon dispersion relation:

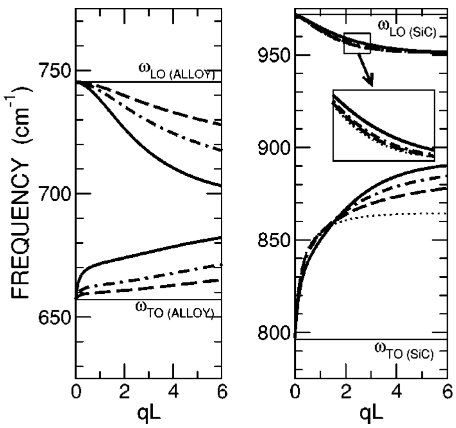

FIG. 2. Phonon's dispersion relation as a function of the dimensionless wave vector qL for abrupt $3C$-SiC/Si and nonabrupt $Si/Si_x(3C\text{-}SiC)_{1-x}/3C$-SiC heterojunctions. Here the dotted lines are related to the abrupt interface case, while the dashed, dotted dashed, and solid lines describe the nonabrupt case for interface thicknesses d_2 equal to 0.5, 1.0, and 2.5 nm, respectively. Observe the *new* optical phonon's mode in the left-hand side of the spectrum.

$$\exp(-2\alpha_2 d_2)=\prod_i \frac{\gamma_i^+\beta_i^+ + \gamma_i^-\beta_i^-\exp(-2\alpha_i d_i)}{\gamma_i^-\beta_i^+ + \gamma_i^+\beta_i^-\exp(-2\alpha_i d_i)}, \quad (7)$$

where

$$\gamma_i^{\pm}=\alpha_i\epsilon_{2\perp}\pm\alpha_2\epsilon_{i\perp}, \quad (8)$$

$$\beta_i^{\pm}=\alpha_v\epsilon_{i\perp}\pm\alpha_i\epsilon_v. \quad (9)$$

Here $i=1$ is assigned to the $3C$-SiC layers of thickness $d_1=L_{3C\text{-SiC}}$, $i=2$ to the alloy $(3C\text{-SiC})_x(\mathrm{Si})_{1-x}$ of thickness $d_2=L_{(3C\text{-SiC})_x(\mathrm{Si})_{1-x}}$, and $i=3$ to the Si layers of thickness $d_3=L_{\mathrm{Si}}$. The wavevector α_v associated to the vacuum is $\alpha_v^2=q^2-\omega^2/c^2$ and

$$\alpha_j^2=q^2\frac{\epsilon_{j\perp}}{\epsilon_{j\parallel}}-\epsilon_{j\perp}\frac{\omega^2}{c^2} \quad (10)$$

for $j=1,2,3$. The thickness $d_2=L_{(3C\text{-SiC})_x(\mathrm{Si})_{1-x}}$ determines the role of the interface in the phonon dispersion relation.

On the other hand, for the case of the abrupt $3C$-SiC/Si heterojunction whose width is $L=d_1+d_3$, the phonon dispersion relation is given by

$$\exp(-2\alpha_3 d_3)=\left(\frac{\beta_3^+}{\beta_3^-}\right)\frac{\gamma_1^+\beta_1^+ + \gamma_1^-\beta_1^-\exp(-2\alpha_1 d_1)}{\gamma_1^-\beta_1^+ + \gamma_1^+\beta_1^-\exp(-2\alpha_1 d_1)}. \quad (11)$$

Considering the abrupt $3C$-SiC/Si heterojunction of width $L=10$ nm, the phonon dispersion relation presents higher symmetric (top) and antisymmetric (bottom) branches located between the ω_{LO} (SiC) and ω_{TO} (SiC) phonon's frequencies. This is shown by the dotted lines in the right-hand side of Fig. 2, which depicts the high-frequency spectrum against the dimensionless wave vector qL. The physical parameters used for Si in the calculations were $\epsilon_\infty=11.7$, $\omega_{LO}=\omega_{TO}=518.02$ cm^{-1}, while for SiC we used $\epsilon_\infty=6.7$, $\omega_{LO}=972$ cm^{-1}, and $\omega_{TO}=796$ cm^{-1}.

Now, taking into account the existence of a nonabrupt interface, there is a split in energy up to 25 cm^{-1} as compared with the abrupt case. This can be observed in Fig. 2, where are depicted the behavior of the phonons branches of nonabrupt $3C$-SiC/Si heterojunctions with interface thickness d_2 equal to 0.5 nm (dashed lines), 1.0 nm (dotted dashed lines), and 2.5 nm (solid lines). The higher symmetric and antisymmetric phonons branches shift to bigger frequencies, the former very weakly (~ 1 cm^{-1}, the lines assigned to each interface are collapsed in this case as shown by the inset in the right-hand side of Fig. 2), and the latter strongly (~ 25 cm^{-1} when $qL=6$). When the interface becomes thicker, the overall effect is to increase the shifts of all the symmetric and antisymmetric phonons branches. Observe that the nonabrupt interface has small effect in the frequency of the highest-frequency phonon mode.

The left-hand side of Fig. 2 clearly shows the most dramatic change due to the nonabrupt interfaces: the rise of *new* lower antisymmetric (top) and symmetric (bottom) optical-phonon modes between the ω_{LO} and ω_{TO} phonon's frequencies of the $(3C\text{-SiC})_x(\mathrm{Si})_{1-x}$ alloy, which were calculated as an interpolation of the frequencies of the constituents (see Fig. 1). The frequency of these new nonabrupt interface related modes shifts strongly for high qL when the heterojunction thickness L increases (~ 20 cm^{-1} for a 10 nm wide heterojunction). Another interesting feature of the phonon spectrum is that the gap between the modes decreases as the interface becomes thicker. This happens because the interface becomes more bulky than the constituents of the heterojunction.

The behavior of the phonon branches with the width L of the abrupt (dotted lines) and nonabrupt $3C$-SiC/Si heterojunctions with interface thickness d_2 equal to 0.5 nm (dashed lines), 1.0 nm (dotted dashed lines), and 2.5 nm (solid lines) for a fixed value of the dimensionless wave vector $qL=3$ is presented in Fig. 3. When $L<15$ nm, the dependence of the

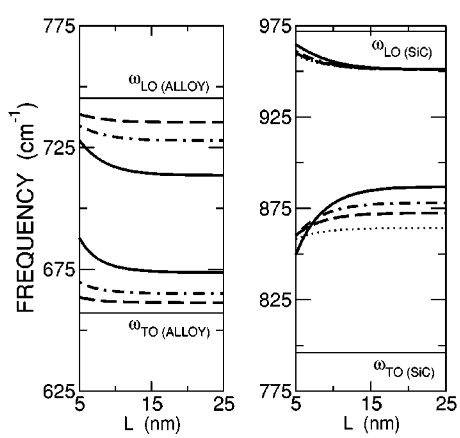

FIG. 3. Phonon's dispersion relation as a function of the heterojunction width (in nm) for a fixed value of the dimensionless wave vector qL (here considered equal to 3). As in Fig. 3, the dotted lines represent the abrupt case, while the dashed, dotted dashed, and solid lines describe the nonabrupt case for interface thicknesses d_2 equal to 0.5, 1.0, and 2.5 nm, respectively.

phonon branches on the heterojunction width is shown to be stronger when the nonabrupt interfaces are thicker; however, when L becomes larger than 15 nm, the frequency of the phonons becomes more bulky, with no more appreciably changes. This suggest that nonabrupt interface effects are more important that strain effects on shifting the Raman spectra of 3C-SiC/Si heterojunctions when they are thin, i.e., with width $L<15$ nm. As a matter of fact, experimental results have assigned to strain effects shifts of the Raman peaks smaller than 5 cm^{-1} in thick 3C-SiC/Si(100) heterojunctions,[14,15] while the present results are pointing to the existence of nonabrupt interface related shifts that can be four times bigger if the 3C-SiC/Si(100) heterojunctions are thinner than 15 nm.

In conclusion, we have demonstrated strong interface related frequency shifts of lower-frequency phonon modes in 3C-SiC/(3C-SiC$)_x$(Si$)_{1-x}$/Si heterojunctions, as well as the existence of new modes, which were observed in the (3C-SiC$)_x$(Si$)_{1-x}$ related frequency range. As the distribution of strain between the different layers strongly depends on the geometry of the structures and on the nature of the buffer layer, our work points out to the limitation of measuring strain in 3C-SiC/Si heterostructures through analysis of Raman spectra without taking into account the role of nonabrupt interfaces.

The authors would like to acknowledge the financial support provided by the National Research Council (CNPq) through the NanoSemiMat Project (Grant No. 550.015/01-9), CNPq, and CAPES/PROCAD.

*Email address: eudenilson@dfte.ufrn.br

[1] M.A. Stroscio and M. Dutta, *Phonons in Nanostructures* (Cambridge University Press, Cambridge, 2001).
[2] J.R. Arthur, Surf. Sci. **500**, 189 (2002).
[3] G. Belenky, M. Dutta, V.B. Gorfinkel, G.I. Haddad, G.J. Iafrate, K.W. Kim, S. Luryi, M.A. Stroscio, J.P. Sun, H.B. Teng, and SeGi Yu, Physica B **263-264**, 462 (1999).
[4] M.V. Kisin, M.A. Stroscio, G. Belenky, V.B. Gorfinkel, and S. Luryi, J. Appl. Phys. **83**, 4816 (1998).
[5] H.B. Teng, J.P. Sun, G.I. Haddad, M.A. Stroscio, SeGi Yu, and K.W. Kim, J. Appl. Phys. **84**, 2155 (1998).
[6] E.C. Ferreira, E.L. Albuquerque, J.A.P. da Costa, P.W. Mauriz, and V.N. Freire, Physica E (Amsterdam) **17C**, 270 (2003); K.S. Chang, E.H. Li, and M.C.Y. Chang, IEEE J. Quantum Electron. **34**, 157 (1998).
[7] K.W. Goossen, J.E. Cunningham, and W.Y. Jan, Appl. Phys. Lett. **57**, 2582 (1990); J. Feldmann, K.W. Goossen, D.A.B. Miller, A.M. Fox, J.E. Cunningham, and W.Y. Jan, *ibid.* **59**, 66 (1991); K.W. Goossen, J.E. Cunningham, M.D. Williams, F.G. Storz, and W.Y. Jan, Phys. Rev. B **45**, 13 773 (1992); I. Brener, W.H. Knox, K.W. Goossen, and J.E. Cunningham, Phys. Rev. Lett. **70**, 319 (1993).
[8] C.A. Zorman, A.J. Fleischman, A.S. Dewa, M. Mehregany, C. Jacob, S. Nishino, and P. Pirouz, J. Appl. Phys. **78**, 5136 (1995).
[9] K. Yasui, K. Asada, T. Maeda, and T. Akahane, Appl. Surf. Sci. **175-176**, 495 (2001).
[10] J. Hofmann, S. Veprek, and J. Heindl, J. Appl. Phys. **85**, 2652 (1999).
[11] Y. Ikoma *et al.*, Appl. Phys. Lett. **75**, 3977 (1999).
[12] T. Matsumoto, M. Kiuchi, S. Sugimoto, and S. Goto, Surf. Sci. **494**, 426 (2001).
[13] Z.C. Feng, W.W. Choyke, and J.A. Powell, J. Appl. Phys. **64**, 6827 (1988).
[14] S. Rohmfeld, M. Hundhausen, L. Ley, C.A. Zorman, and M. Mehregany, J. Appl. Phys. **91**, 1113 (2002).
[15] L.A. Falkovsky, J.M. Bluet, and J. Camassel, Phys. Rev. B **57**, 11 283 (1998).
[16] J. Zhu, S. Liu, and J. Liang, Thin Solid Films **368**, 307 (2000).
[17] E.F. Bezerra, V.N. Freire, A.G. Souza Filho, J. Mendes Filho, V. Lemos, Y. Ikoma, F. Watanabe, and T. Motooka, Appl. Phys. Lett. **77**, 4316 (2000).
[18] G. Yu, K.W. Kim, M.A. Stroscio, G.J. Iafrate, J.P. Sun, and G.I. Haddad, J. Appl. Phys. **82**, 3363 (1997).
[19] A. Fainstein, P. Etchegoin, M.P. Chamberlain, M. Cardona, K. Totemeyer, and K. Ebert, Phys. Rev. B **51**, 14 448 (1995); A.J. Shields, M.P. Chamberlain, M. Cardona, and K. Ebert, *ibid.* **51**, 17 728 (1995).
[20] W. Duan, J-L. Zhu, and B-L. Gu, Phys. Rev. B **49**, 14 403 (1994); B-L. Gu, W. Duan, S. Xiong, and Y. Guo, *ibid.* **54**, 16 983 (1996).
[21] T. Hatayama, N. Tanaka, T. Fuyuki, and H. Matsunami, J. Electron. Mater. **26**, 160 (1997).
[22] K. Eberl, S.S. Iyer, J.C. Tsang, M.S. Goorsky, and F.K. Legoues, J. Vac. Sci. Technol. B **10**, 934 (1992).
[23] F. Wischmeyer, W. Wondrak, D. Leidich, and E. Niemann, Mater. Sci. Eng., B **61-62**, 563 (1999).
[24] S. Komirenko, K.W. Kim, M.A. Stroscio, and M. Dutta, Phys. Rev. B **59**, 5013 (1999).